Inorg. Chem. **2004**, *43*, 1770–1778

Outer Sphere Perturbation of Delocalized Mixed-Valence Complexes

Mousa Al-Noaimi,[†] Glenn P. A. Yap,[‡] and Robert J. Crutchley*[,†]

Ottawa-Carleton Chemistry Institute, Carleton University, 1125 Colonel By Drive, Ottawa, Ontario, Canada K1S 5B6, and University of Ottawa, Ottawa, Ontario, Canada K1N 6N5

Received August 7, 2003

The complexes $[\{Ru(ttp)(bpy)\}_2(\mu\text{-adpc})][PF_6]_2$ and $[\{Ru(ttp)(bpy)\}_2(\mu\text{-dicyd})][PF_6]_2$, where ttp is 4-toluene-2,2′:6′,2″-terpyridine, bpy is 2,2′-bipyridine, $adpc^{2-}$ is azodi(phenylcyanamide), and $dicyd^{2-}$ is 1,4-dicyanamidebenzene, were prepared and characterized by IR and NIR, vis spectroelectrochemistry, and cyclic voltammetry. The crystal structure of the complex, $[\{Ru(ttp)(bpy)\}_2(\mu\text{-adpc})][PF_6]_2 \cdot 6DMF$, revealed a planar bridging $adpc^{2-}$ ligand with the cyanamide groups adopting an *anti* configuration. IR and comproportionation data are consistent with delocalized mixed-valence complexes, and a spectroscopic analysis assuming C_{2h} microsymmetry leads to a prediction of multiple MMCT transitions with the lowest energy transition equal to the resonance exchange integral for the mixing of ruthenium donor and acceptor orbitals with a bridging ligand orbital (the preferred superexchange pathway). The solvent dependence of the MMCT band energy that is seen for $[\{Ru(ttp)(bpy)\}_2(\mu\text{-adpc})]^{3+}$ is due to a ground state weakening of metal–metal coupling because of solvent donor interactions with the acceptor azo group of the bridging ligand.

Mixed-valence complexes have been known for many years[1,2] with the vast majority of studies performed on symmetric ruthenium valence-trapped systems in which metal ions are joined by a single bridging ligand (BL), possessing identical coordination spheres but differing only by the presence of an extra electron.

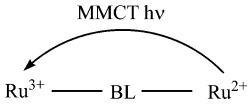

Electron transfer between the Ru ions of this complex can be induced thermally or photochemically (metal-to-metal charge-transfer MMCT), and indeed, the conceptual framework to understand mixed-valence properties[3] owes much to that which forms the basis of the Marcus theory of electron transfer.[4] The mixed-valence properties of these systems depend greatly on the extent of metal−metal coupling, and three cases have been suggested,[5] classes I, II, and III, to characterize no coupling, weak coupling, or very strong coupling cases, respectively. For a complex to be considered class III, there must be no thermal barrier to electron transfer between metal ions, and so, the electron transfer rate is equivalent to electron mobility within an orbital. Both ruthenium ions of a class III system formally have a partial oxidation state of 2.5, and an allowed MMCT transition must result in an electron density distribution resembling that of the ground state of the valence-trapped case to result in a transition dipole moment.

There have been few systematic investigations of the properties of class III compared to class II mixed-valence complexes, but this is changing with the need to understand and recognize the transition between class II and III properties. A recent review by Meyer et al.[6] examined this issue and provided clear spectroscopic evidence for the presence of metal centered transitions arising out of low coordination symmetry in the same region as MMCT transitions and suggested that the high energy asymmetry in band envelope that is observed in the MMCT transitions of some strongly coupled complexes is not a result of class III properties but the presence of these metal centered transitions.

* To whom correspondence should be addressed. E-mail: robert_crutchley@carleton.ca.
† Carleton University.
‡ University of Ottawa. Current location: University of Delaware.

(1) Creutz, C. *Prog. Inorg. Chem.* **1983**, *30*, 1.
(2) Crutchley, R. J. *Adv. Inorg. Chem.* **1994**, *41*, 273.
(3) Hush, N. S. *Prog. Inorg. Chem.* **1967**, *8*, 391.
(4) Marcus, R. A. *J. Chem. Phys.* **1956**, *24*, 966. (b) Marcus, R. A. *J. Chem. Phys.* **1957**, *26*, 867. (c) Marcus, R. A. *J. Chem. Phys.* **1957**, *26*, 872.
(5) Robin, M. B.; Day, P. *Adv. Inorg. Chem. Radiochem.* **1967**, *10*, 247.
(6) Demadis, K. D.; Hartshorn, C. M.; Meyer, T. J. *Chem. Rev.* **2001**, *101*, 2655.

10.1021/ic0349454 CCC: $27.50
Published on Web 02/07/2004

In addition, the effect of solvent on the mixed-valence properties has often been used to discriminate between class II or III complexes.[1,2,7] However, Meyer points out that if thermal electron transfer between donor and acceptor metal ions is greater than the rate of solvent relaxation 10^{12} s^{-1}, the mixed-valence properties of the complex would appear solvent independent even though on the electronic time scale 10^{15} s^{-1} the odd electron is trapped on one metal ion. For such systems at the borderline of class II and III behavior and possessing intermediate properties, Meyer proposed the new classification class II−III.[6]

In order to distinguish between class II and III mixed-valence complexes, a measure of metal−metal coupling is needed. For a mixed-valence complex, one measure is provided by the free energy of comproportionation, ΔG_c, according to the comproportionation equilibrium

$$\mathrm{Ru(III,III)} + \mathrm{Ru(II,II)} \overset{K_c}{\longleftrightarrow} 2\mathrm{Ru(III,II)} \qquad (1)$$

that also defines the comproportionation constant, K_c. For the sake of simplicity, we will denote the mixed-valence state Ru(III,II) for the complexes of this study even though a more appropriate class III designation would be $\mathrm{Ru(II^{1}/_{2},II^{1}/_{2})}$.

ΔG_c may be determined electrochemically by using cyclic voltammetry, where the difference between metal centered redox couple potentials, $\Delta E = \mathrm{Ru_2} - \mathrm{Ru_1}$, can be related to the free energy of comproportionation via the Nernst equation.

$$[\mathrm{Ru(III,III)}] \overset{\mathrm{Ru_2}}{\longleftrightarrow} [\mathrm{Ru(III,II)}] \overset{\mathrm{Ru_1}}{\longleftrightarrow} [\mathrm{Ru(II,II)}] \qquad (2)$$

For the majority of mixed-valence complexes, the magnitude of ΔG_c can be adequately described by four factors:[8]

$$\Delta G_c = \Delta G_s + \Delta G_e + \Delta G_i + \Delta G_r \qquad (3)$$

In eq 3, ΔG_s reflects the statistical distribution of the comproportionation equilibrium, ΔG_e accounts for the electrostatic repulsion of the two like-charged metal centers, ΔG_i is an inductive factor dealing with competitive coordination of the bridging ligand by the metal ions, and ΔG_r is the free energy of resonance exchange. If the oxidized form of the complex, Ru(III,III), experiences antiferromagnetic exchange, the term ΔG_{ex} must be included.[9] This term measures the stabilizing influence antiferromagnetic exchange has upon a reactant complex in eq 1 and, thus, is of opposite sign to the remaining terms in eq 3. In addition, a recent study[10] has shown that ion pairing can have a dramatic influence on comproportionation equilibrium and the ion pairing factor ΔG_{ip} either increases or decreases its magnitude depending on the charge of the complexes in eq 1. Including these terms in eq 3 yields

$$\Delta G_c = \Delta G_s + \Delta G_e + \Delta G_i + \Delta G_r + \Delta G_{ex} + \Delta G_{ip} \qquad (4)$$

We have shown that it is possible to extract the value of ΔG_r from comproportionation data of strongly coupled mixed-valence complexes and hence determine the free energy of resonance exchange per mixed-valence complex, $\Delta G_r' = 0.5\Delta G_r$.[9] The actual measure of metal−metal coupling is given by the resonance exchange integral (or metal−metal coupling element) H_{ad} which for strongly coupled symmetric class III systems is related to $\Delta G_r'$ by[11]

$$\Delta G_r' = H_{ad} - \Delta G_{th} \qquad (5)$$

where ΔG_{th} is the activation energy for thermal electron transfer in the absence of metal−metal coupling. The complexes of this study have similar coordination spheres and charges so that the differences between values of ΔG_s, ΔG_e, ΔG_i, ΔG_{ip}, and ΔG_{th} between the complexes are small.[12] This means that differences in ΔG_c between the complexes actually reflect differences in ΔG_r and ΔG_{ex}.

Another measure of metal−metal coupling can be derived from MMCT band energy. According to the two-state Hush model of mixed-valence complexes, the resonance exchange integral H_{ad} for class III systems is simply related to the energy of the MMCT band, E_{op}, by

$$E_{op} = 2H_{ad} \qquad (6)$$

When there is significant mixing of ligand and metal donor and acceptor orbitals, a three-state description is more appropriate[13] in which case the MMCT transition occurs between nonbonding and antibonding orbitals and the band energy is equivalent to H_{ad}.

For this study, we have prepared the complexes $[\{\mathrm{Ru(ttp)(bpy)}\}_2(\mu\text{-adpc})][\mathrm{PF_6}]_2$ and $[\{\mathrm{Ru(ttp)(bpy)}\}_2(\mu\text{-dicyd})][\mathrm{PF_6}]_2$, where ttp is 4-toluene-2,2′:6′,2″-terpyridine, bpy is 2,2′-bipyridine, $\mathrm{adpc^{2-}}$ is azodi(phenylcyanamide), and $\mathrm{dicyd^{2-}}$ is 1,4-dicyanamidebenzene. In earlier studies, we prepared the analogous terpyridine complexes[14,15] but noted their poor solubility in all but the strongest donor solvents. Greatly improved solubility was found for the analogous complexes

(7) Creutz, C.; Chou, M. H. *Inorg. Chem.* **1987**, *26*, 2995.
(8) Richardson, D. E.; Taube, H. *Coord. Chem. Rev.* **1984**, *60*, 107.
(9) Evans, C. E. B.; Naklicki, M. L.; Rezvani, A. R.; White, C. A.; Kondratiev, V. V.; Crutchley, R. J. *J. Am. Chem. Soc.* **1998**, *120*, 13096.
(10) Barrière, F.; Camire, N.; Geiger, W. E.; Mueller-Westerhoff, U. T.; Sanders, R. *J. Am. Chem. Soc.* **2002**, *124*, 7262.
(11) Brunschwig, B. S.; Sutin, N. *Coord. Chem. Rev.* **1999**, *187*, 233.
(12) This assumption is only acceptable when ΔG_r and ΔG_{ex} are large and the difference between ΔG_c for the complexes ($\Delta\Delta G_c$) is also large. For the complexes of this study, the experimental $\Delta\Delta G_c$ is equal to 2700 cm^{-1} in nitromethane. We show in this study that when corrected for ΔG_{ex}, $\Delta\Delta G_c$ rises dramatically to 6000 cm^{-1}. ΔG_e for $[\{\mathrm{Ru(ttp)(bpy)}\}_2(\mu\text{-dicyd})]^{3+}$ in nitromethane is calculated (see ref 9) to be 250 cm^{-1} whereas that for $[\{\mathrm{Ru(ttp)(bpy)}\}_2(\mu\text{-adpc})]^{3+}$ in nitromethane is 180 cm^{-1}. The value of ΔG_i for the complexes is not known; however, that of $[\{(\mathrm{NH_3})_5\mathrm{Ru}\}_2(\mu\text{-dicyd})]^{3+}$ has been estimated to be between 120 and 320 cm^{-1} (see ref 9). We expect that the difference in ΔG_i between complexes is of the same magnitude and small. The difference between thermal barriers to electron transfer can be calculated by assuming that the inner sphere contributions are the same for both complexes and that the outer sphere contributions can be calculated by using the dielectric continuum model[1] and complex spheres of 5 Å (see: Brown, G. M.; Sutin, N. *J. Am. Chem. Soc.* **1979**, *101*, 883). This calculation gave a difference in ΔG_{th} for 13 and 18 Å metal−metal separation of 300 cm^{-1} for the complexes in nitromethane. ΔG_s is constant, and as we show later, the symmetric splitting of the Ru(III/II) couples of $[\{\mathrm{Ru(ttp)(bpy)}\}_2(\mu\text{-adpc})]^{4+}$ suggests that ΔG_{ip} is not important.
(13) Brunschwig, B. S.; Creutz, C.; Sutin, N. *Chem. Soc. Rev.* **2002**, *31*, 168.

of the ttp ligand, and so, we have performed comprehensive cyclic voltammetry and IR and NIR−vis spectroelectrochemical studies of these complexes in a range of solvents. The data are consistent with a class III designation for the complexes' mixed-valence states.

Experimental Section

Materials. All of the reagents and solvents used were reagent grade or better. The solvents, nitromethane (NM), propylene carbonate (PC), dimethyl sulfoxide (DMSO), and *N*,*N*′-dimethylformamide (DMF), were dried with anhydrous alumina and vacuum distilled. Acetonitrile (AN) was dried over phosphorus pentoxide and vacuum distilled. Acetone (AC), nitrobenzene (NB), and 1,2-dichloroethane (DCE) were used as received. Tetrabutylammonium hexafluorophosphate (TBAH), purchased from Aldrich, was twice recrystallized from 1:1 ethanol/water and vacuum-dried at 110 °C. Thallium salts (*caution: highly toxic*) of 2,3,5,6-tetrachlorophenylcyanamide (Cl_4pcyd^-),[16] 4,4′-azodi(phenylcyanamide) dianion ($adpc^{2-}$),[15] and 1,4-dicyanamidebenzene ($dicyd^{2-}$)[14] and 4-toluene-2,2′:6′,2″-terpyridine (ttp)[17] were prepared according to literature methods. The reagent complex $Ru(ttp)Cl_3$ was synthesized by following the literature preparation of the analogous terpyridine complex[18] and was used without further purification.

Synthesis of [Ru(ttp)(bpy)Cl][PF$_6$]·2DMF. $Ru(ttp)Cl_3$ (642 mg, 1.2 mmol) and 2.2′-bipyridine (197 mg, 1.2 mmol) were dissolved in 150 mL of 4:1 water/ethanol and refluxed for 5 h, and then, LiCl (500 mg) was added. After refluxing for an additional 1 h, NH_4PF_6 (200 mg) was added, the reaction solution volume was reduced to about 50 mL, and the solution was stored in the fridge overnight. The precipitated crude product was filtered off and then purified by column chromotography by using grade III alumina type WA-I (Sigma), with a 2:1 mixture of tolune/ acetonitrile as eluent. The main deep purple band was collected and the solvent evaporated into dryness by rotary evaporation. The product was recrystallized by the diffusion of ether into a saturated *N*,*N*′-dimethylformamide (DMF) solution of the complex. Yield 0.62 mg (82%). Anal. Calcd for $C_{38}H_{39}N_7O_2F_6PClRu$: C, 50.31; H, 4.33; N, 10.81. Found: C, 50.15; H, 4.61; N, 11.21. ^{1}H NMR: methyl protons, 2.45 (1H, singlet); ttp and bpy protons, 10.09 (1H, doublet); 9.16 (2H, singlet); 8.93 (3H, triplet); 8.64 (1H, doublet); 8.35 (1H, triplet of doublet); 8.24 (2H, doublet); 8.06 (1H, triplet); 8.01 (2H, triplet of doublet); 7.94 (1H, singlet); 7.77 (1H, triplet of doublet); 7.62 (2H, doublet); 7.51 (2H, doublet); 7.42 (1 H, doublet); 7.38 (2H, triplet); 7.07 (1H, triplet).

Synthesis of [Ru(ttp)(bpy)(Cl$_4$pcyd)][PF$_6$]·2DMF. [Ru(ttp)-(bpy)Cl][PF_6] (0.38 g, 0.51 mmol) was dissolved in 100 mL of DMF in a 250 mL round-bottom flask. $TlCl_4pcyd$ (0.235 g, 0.51 mmol) was added. The deep red solution was refluxed for 18 h, and the reaction mixture was then chilled to −20 °C. The precipitate, TlCl, was filtered through celite. Ether (500 mL) was added to the solution in order to precipitate the crude product, which was then collected by suction filtration. Recrystallization was achieved by the slow diffusion of ether into a saturated solution of the crude complex in DMF. Yield 0.46 g (81%). Anal. Calcd for $RuN_9C_{45}H_{40}PF_6O_2Cl_4$: C, 47.97; H, 3.58; N, 11.19. Found: C, 48.25; H, 3.79; N, 11.32. UV−vis in DMF [λ_{max}/nm (ϵ_{max}/dm^3 mol^{-1} cm^{-1})], 503 (1.2×10^4). ^{1}H NMR (400 MHz) in dimethyl sulfoxide-d_6, relative to TMS at 0.00 ppm; methyl protons at 2.48 (3H, singlet); ttp and bpy protons at 9.64 (1H, doublet), 9.29 (2H, singlet); 9.06 (2H, doublet); 8.97 (1H, doublet); 8.71 (1H, doublet); 8.42 (1H, triplet); 8.29 (2H, triplet); 8.12 (3H, multiplet); 7.88 (1H, triplet); 7.50 (2H, doublet); 7.58 (1H, doublet); 7.53 (1H, doublet); 7.48 (2H, triplet); 7.17 (1H, triplet); 5.87 (1H, singlet). ν(NCN), 2167 cm^{-1}.

Synthesis of [{Ru(ttp)(bpy)}$_2$(μ-adpc)][PF$_6$]$_2$. To a solution of [Ru(ttp)(bpy)Cl][PF_6] (0.673 g, 0.89 mmol) dissolved in 100 mL of DMF was added Tl_2(adpc) (0.30 g, 0.45 mmol) and the reaction mixture refluxed for 3 days. The solution was then chilled to −20 °C and filtered with celite to remove TlCl precipitate. The filtrate was concentrated to 20 mL by rotary evaporation, and then, 600 mL of ether was added to precipitate the crude product. This was filtered off, dissolved in 60 mL of acetonitrile/toluene (3:1), and purified by chromatography by using a 50 cm × 3 cm diameter column containing 250 g grade(V) alumina (Brockmann I, weakly acidic 150 mesh). Elution with acetonitrile/toluene (3:1) yielded two bands which were spectroscopically identified as unreacted reagents, $[Ru(ttp)(bpy)Cl]^+$ and $adpc^{2-}$. Elution with acetonitrile and acetonitrile/methanol (4:1) gave the desired dinuclear complex which, after evaporation to dryness, was dissolved in 10 mL of dimethylformamide and filtered through celite. To the filtrate was added excess aqueous NH_4PF_6, precipitating the dinuclear complex. Recrystallization was achieved by the slow diffusion of ether into saturated solution of the complex in dimethylformamide. Yield after vacuum-drying 470 mg (55%). Anal. Calcd for $C_{78}H_{58}N_{16}F_{12}P_2Ru_2$: C, 54.74; H, 3.42; N, 13.09. Found: C, 54.35; H, 3.36; N, 13.11. ^{1}H NMR: methyl protons at 2.45 (6H, singlet); phenyl protons for $adpc^{2-}$ bridging ligand at 6.03 (4H, doublet) and 7.19 (4H, doublet); ttp and bpy protons at 9.66 (2H, doublet); 9.25 (4H, singlet); 9.02 (4H, doublet); 8.96 (2H, doublet); 8.69 (2H, doublet); 8.40 (2H, triplet); 8.26 (4H,doublet); 8.11 (6H, triplet); 7.85 (2H, triplet); 7.69 (4H, multiplet); 7.55 (H, doublet); 7.49 (H, doublet); 7.46 (H, doublet); 7.15 (2H, triplet). IR: ν(NCN) 2171 cm^{-1}.

Synthesis of [{Ru(ttp)(bpy)}$_2$(μ-dicyd)][PF$_6$]$_2$. The procedure is identical to the above synthesis except that Tl_2(dicyd) (242 mg, 0.45 mmol) was used instead of Tl_2(adpc) and the mixture was refluxed under argon atmosphere. Yield 364 mg (43%). Anal. Calcd for $C_{72}H_{54}N_{14}P_2F_{12}Ru_2$: C, 53.80; H, 3.39; N, 12.20. Found: C, 53.44; H, 3.22; N, 12.24. ^{1}H NMR: methyl protons, 2.45 (6H, singlet); $dicyd^{2-}$ phenyl protons, 5.45 (4H, singlet); ttp and bpy protons, 9.62 (2H, doublet); 9.16 (4H, singlet); 8.93 (6H, doublet); 8.66 (2H, doublet); 8.36 (2H, triplet); 8.20 (4H, doublet); 8.07 (2H, doublet); 8.01 (4H, triplet); 7.80 (2H, triplet); 7.64 (4H, doublet); 7.46 (6H, triplet) 7.39 (4H, triplet); 7.09 (2H, triplet). IR: ν(NCN), 2138 cm^{-1}.

Crystallography. Thin plates of [{Ru(ttp)(bpy)}$_2$(μ-adpc)][PF_6]$_2$·6DMF were grown by slow diffusion of diethyl ether into a *N*,*N*′-dimethylformamide (DMF) solution of complex. The data were collected on a 1K Siemens Smart CCD using Mo Kα radiation (λ = 0.71073 Å) at 203(2) K using an ω-scan technique and corrected for absorptions using equivalent reflections.[19] No symmetry higher than triclinic was observed, and solution in the centric space group option yielded chemically reasonable and computationally stable results of refinement. The structure was solved by direct methods and refined with full-matrix least-squares procedures. The molecular

(14) Rezvani, A. R.; Evans, C. E. B.; Crutchley, R. J. *Inorg. Chem*. **1995**, *34*, 4600.
(15) Mosher, P. J.; Yap, G. P. A.; Crutchley, R. J. *Inorg. Chem*. **2001**, *40*, 1189.
(16) Crutchley, R. J.; McCaw, K.; Lee, F. L.; Gabe, E. J. *Inorg. Chem.* **1990**, *29*, 2576.
(17) Leigghio, R.; Potvin, P. G.; Lever, A. B. P. *Inorg. Chem*. **2001**, *40*, 5485.
(18) Takeuchi, K. J.; Thompson, M. S.; Pipes, D. W.; Meyer, T. J. *Inorg. Chem*. **1984**, *23*, 1845.
(19) Blessing, R. *Acta Crystallogr*. **1995**, *A51*, 33.

cation is located at an inversion center. Six molecules of DMF are cocrystallized in the unit cell. Anisotropic refinement was performed on all non-hydrogen atoms. All hydrogen atoms were calculated. Scattering factors are contained in the SHELXTL 5.1 program library.

Equipment. UV−vis spectroscopy was performed on a Cary 5 UV−vis−NIR spectrophotometer. IR spectra were taken with a BOMEM Michelson-120 FT-IR spectrophotometer (KBr disks). ^{1}H NMR data in ppm relative to TMS (0.00 ppm) were determined from dimethyl sulfoxide-d_6 solutions by using a Bruker AMX-400 spectrometer. Cyclic voltammetry was performed using a BAS CV-27 voltammograph, and plotted on a BAS XY recorder. The sample cell consisted of a double walled glass crucible with an inner volume of ~15 mL which was fitted with a Teflon lid incorporating a three-electrode system and argon bubbler. The cell temperature was maintained at (25.0 ± 0.1) °C by means of a Haake D8 recirculating bath. BAS 2013 Pt electrodes (1.6 mm diameter) were used as the working and counter electrodes. A silver wire functioned as a pseudo-reference-electrode, and the electrolyte was 0.1 M TBAH. Ferrocene ($E°$ = 0.665 V versus NHE) was used as an internal reference.[20] An OTTLE cell was used to perform the spectroelectrochemistry.[21] The cell had interior dimensions of roughly 1 × 2 cm^2 with a path length of 0.2 mm and was fitted with a silver/silver chloride reference electrode. For visible NIR studies, ITO (indium−tin oxide) coated glass served as working and counter electrodes and was purchased from Delta Technologies. For IR studies, the working electrode was gold mesh (500 lines/inch, 60% transmittance) purchased from Buckbee-Mears. Elemental analyses were performed by Canadian Microanalytical Services.

Results

The complexes of this study were synthesized in good yields by the metathesis reaction of [Ru(ttp)(bpy)Cl]$^+$ with the thallium salts of Cl_4pcyd^-, dicyd^{2-}, or adpc^{2-} in refluxing DMF and purified by column chromatography on alumina. These Ru(II) complexes are air stable and can be readily recrystallized. We attempted to obtain crystals of the dinuclear complex cation, [{Ru(ttp)(bpy)}$_2$(μ-dicyd)]$^{2+}$, by using various counterions and solvent conditions but were unsuccessful. Nevertheless, we were able to obtain crystals of the analogous adpc^{2-} complex.

Deep red-brown plates of the dinuclear Ru(II) complex, [{Ru(ttp)(bpy)}$_2$(μ-adpc)][PF$_6$]·6DMF, that were suitable for crystallography were grown by diffusion of ether into a solution of the complex in DMF. Crystallographic data and bond lengths and angles are reported in Tables 1 and 2. An ORTEP drawing of the complex cation is shown in Figure 1. The Ru(II) ion occupies a pseudo-octahedral coordination sphere of nitrogen donor atoms where the cyanamide group of the adpc^{2-} bridging ligand is *trans* to a pyridine moiety of the bipyridine ligand. The adpc^{2-} ligand is approximately planar with the cyanamide groups in an *anti*-conformation relative to each other and the azo group adopting the more thermodynamically stable *trans* conformation. This conformation of the bridging ligand is essentially identical to that obtained in an earlier study for [{Ru(terpyrdine)(bpy)}$_2$(μ-adpc)][PF$_6$],[15] and indeed, the planar geometry of adpc^{2-} is a common feature of all aromatic cyanamide ligands.[22] The cyanamide group is approximately linear (172.0(7)°) as is the coordination of its terminal nitrogen to Ru(II) (174.3(5)°). In contrast, the crystal structure of [{Ru(terpyridine)(bpy)}$_2$-(μ-adpc)][PF$_6$][15] showed that the coordination of the cyanamide group to Ru(II) was significantly bent with an angle of 164.4(2)°. This difference in Ru−cyanamide bond angle

Table 1. Crystal Data for [{Ru(ttp)(bpy)}$_2$(μ-adpc)][PF$_6$]$_2$·6*N*,*N*′-dimethylformamide

formula	$C_{96}H_{100}F_{12}N_{22}O_6P_2Ru_2$
fw	2150.06 g/mol
cryst syst	triclinic
space group	$P\bar{1}$
unit cell dimensions	*a*, 13.1504(18) Å
	b, 13.4147(18) Å
	c, 14.3338(18) Å
α, β, γ	76.176(3)°
	81.3525(3)°
	79.954(3)°
V	2401.9(6) Å^3
Z	1
calcd *d*	1.486 g/cm^3
cryst dimens	0.20 × 0.10 × 0.02 mm^3
θ range	1.58−28.96°
limiting indices	$-16 \le h \le 16$
	$-17 \le k \le 17$
	$0 \le l \le 15$
reflns collected	8477
unique reflns	7004
abs correction	semiempirical from equivalents
transm range	1.000000−0.757626
R1, wR2 [$I > 2\sigma(I)$][a]	R1 = 0.0619, wR2 = 0.1325
GOF on F^2	1.034

[a] $R1 = \sum||F_o| - |F_c||/\sum|F_o|$, $wR2 = (\sum w(|F_o| - |F_c|)^2/\sum w|F_o|^2)^{1/2}$.

Table 2. Selected Crystal Structure Data for [{Ru(ttp)(bpy)}$_2$(μ-adpc)][PF$_6$]$_2$·6*N*,*N*′-dimethylformamide

Bond Lengths[a]/Å			
Ru−N(1)	2.074(5)	N(6)−C(33)	1.162(7)
Ru−N((2)	1.971(5)	N(7)−C(33)	1.299(8)
Ru−N(3)	2.081(5)	N(7)−C(34)	1.407(8)
Ru−N(4)	2.073(5)	N(8)−C(37)	1.454(9)
Ru−N(5)	2.040(5)	N(8)−N(8A)	1.234(11)
Ru−N(6)	2.049(5)		

Bond Angles[a]/deg			
N(1)−Ru−N(2)	79.9(2)	N(4)−Ru−N(5)	78.7(2)
N(1)−Ru−N(5)	88.4(2)	N(6)−C(33)−N(7)	172.0(7)
N(3)−Ru−N(2)	79.02(2)	C(33)−N(6)−Ru	174.3(5)
N(4)−Ru−N(3)	104.55(19)	C(33)−N(7)−C(34)	120.5(6)
N(5)−Ru−N(2)	99.2(2)	N(8A)−N(8)−C(37)	112.7(9)

[a] Estimated standard deviations are in parentheses.

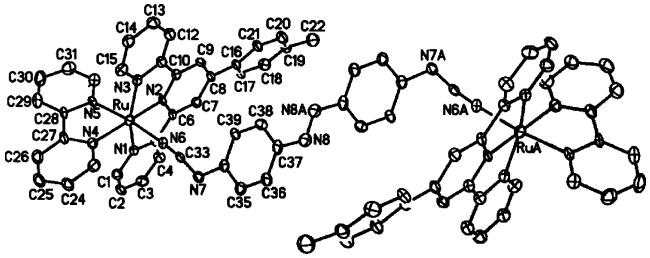

Figure 1. ORTEP drawing of [{Ru(tpp)(bpy)}$_2$(μ-adpc)]$^{2+}$. The counterions, hydrogen atoms, and solvent of crystallization (six DMF molecules) have been ommited for clarity. Ellipsoids are depicted at 30% probability.

(20) Gennett, T.; Milner, D. F.; Weaver, M. J. *J. Phys. Chem.* **1985**, *89*, 2787.
(21) (a) Krejcik, M.; Danek, M.; Hartl, F. *J. Electroanal. Chem.* **1991**, *317*, 179. (b) Evans, C. E. B. Ph.D. Thesis, Carleton University, 1997.
(22) Aquino, M. A. S.; Crutchley, R. J.; Lee, F. L.; Gabe, E. J.; Bensimon, C. *Acta Crystallogr.* **1993**, *C49*, 1543.

Table 3. Solvent Dependent Electrochemical Data[a] Determined for $[\{Ru(ttp)(bpy)\}_2(\mu\text{-adpc})][PF_6]_2$

solvent	Ru_2[b]	Ru_1[c]	ΔE[d]	K_c[e]	L_1[f]	L_2[f]
NM	1.65	0.87	0.78	1.5×10^{13}		
AC	1.52	0.78	0.74	3.2×10^{12}	−1.18	−1.41
PC	1.50	0.77	0.73	2.2×10^{12}	−1.19	−1.46
DMF	1.27	0.58	0.69	4.6×10^{11}	−1.34	−1.64
DMSO		0.83			−1.24	−1.39

[a] Versus NHE, platinum working electrode, 0.1 M TBAH electrolyte, at 25 °C. [b] Ru_2 = Ru(III,III)/Ru(III,II). [c] Ru_1 = Ru(III,II)/Ru(II,II). [d] $\Delta E = Ru_1 - Ru_2$. [e] The comproportionation constant $K_c = 10^{16.91\Delta E}$. [f] Ligand reduction couples L_1 and L_2 of terpyridine and bipyridine ligands, respectively.

Table 4. Redox Couples[a] and Comproportionation Constants for $[\{Ru(ttp)(bpy)\}_2(\mu\text{-dicyd})][PF_6]_2$ as a Function of Solvent

solvent	Ru_1	Ru_2	ΔE	K_c	L_1[f]	L_2[f]
NM	0.79	0.35	0.44	2.8×10^7		
AC	0.79	0.33	0.46	6.0×10^7	−1.16	−1.53
DMF	0.80	0.32	0.48	1.30×10^8	−0.875	−1.175
DMSO	0.0.79	0.35	0.44	2.8×10^7	−0.90	−1.173

[a] Versus NHE, platinum working electrode, 0.1 M TBAH electrolyte, at 25 °C. [b] Ru_2 = Ru(III,III)/Ru(III,II). [c] Ru_1 = Ru(III,II)/Ru(II,II). [d] $\Delta E = Ru_1 - Ru_2$. [e] The comproportionation constant $K_c = 10^{16.91\Delta E}$. [f] Ligand reduction couples L_1 and L_2 of terpyridine and bipyridine ligands, respectively.

may indicate that crystal packing forces are sufficient to overcome the weak π-bonding between Ru(II) and the cyanamide group that would be optimized by a linear coordination mode. Furthermore, while the complex cation in the solid state possesses an inversion center, it seems likely that the complex in solution will be able to access a range of possible conformations of lower symmetry, and this will have relevance to the spectroscopic analysis to follow.

Cyclic voltammetry data for $[\{Ru(ttp)(bpy)\}_2(\mu\text{-adpc})]^{2+}$ in various solvents are shown in Table 3 while the data for $[\{Ru(ttp)(bpy)\}_2(\mu\text{-dicyd})]^{2+}$ are given in Table 4. Also given are comproportionation constants as defined by eq 1. The bpy and ttp ligand reductions in similar complexes occur between −1 and −2 V versus NHE, with the first reduction wave L_1, assigned to ttp (0/−1),[15,23] showing some reversibility. Reduction of the azo group also occurs in this potential range and is an irreversible process.[15]

Cyclic voltammograms showing the Ru(III/II) couples of the mononuclear complex $[Ru(ttp)(bpy)(Cl_4pcyd)][PF_6]$ and the dinuclear complexes $[\{Ru(ttp)(bpy)\}_2(\mu\text{-dicyd})][PF_6]_2$ and $[\{Ru(ttp)(bpy)\}_2(\mu\text{-adpc})][PF_6]_2$, in acetonitrile solution, are shown in Figure 2. The Ru(III/II) couples are generally quasireversible with anodic to cathodic waves separated by approximately 80 mV and largely invariant with scan rate. Reduced reversibility of the most positive Ru(III/II) couple corresponding to Ru(III,III)/Ru(II,III) was noted in some solvents making spectroelectrochemical studies of this couple problematic. The most positive couple seen in Figure 2a,b is assigned to the oxidation of the cyanamide ligand by comparison to the cyclic voltammogram of $[Ru(NH_3)_5(2,3\text{-dichlorophenylcyanamide})]^{2+}$.[24] For $[\{Ru(ttp)(bpy)\}_2(\mu\text{-adpc})][PF_6]_2$, this couple is shifted to more positive potentials because of the electron withdrawing properties of the azo group and so is not seen in Figure 2c.

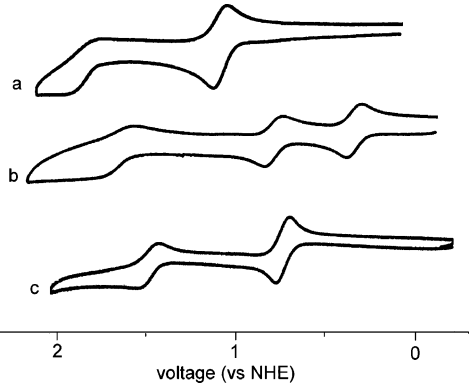

Figure 2. Cyclic voltammogram of (a) $[Ru(ttp)(bpy)(Cl_4pcyd)][PF_6]$, (b) $[\{Ru(ttp)(bpy)\}_2(\mu\text{-dicyd})][PF_6]_2$, and (c) $[\{Ru(ttp)(bpy)\}_2(\mu\text{-adpc})][PF_6]_2$, in acetonitrile, 0.1 M TBAH electrolyte, scan rate 100 mV/s.

The comproportionation constants in Tables 3 and 4 are quite large and indicative of very strong metal−metal coupling. To determine whether these mixed-valence complexes are delocalized or localized systems, infrared spectroelectrochemistry was performed as its time scale (10^{-13} s) gives an almost instantaneous view of the state of a fluxional molecule. An earlier study[25] on mixed-valence polyammine complexes bridged by 1,4-dicyanamide ligands showed that a single ν(NCN) band appeared for the delocalized state while two bands appeared for the valence-trapped state. Interestingly, the ν(NCN) of the cyanamide bound to Ru(II) was at higher frequency than that of cyanamide group bound to Ru(III). This has been ascribed to the polarizability of the cyanamide group and the effect that this has on cyanamide resonance forms.[25]

The IR spectra in the region of the ν(NCN) band for $[\{Ru(ttp)(bpy)\}_2(\mu\text{-dicyd})][PF_6]_2$ in DMSO and for $[\{Ru(ttp)(bpy)\}_2(\mu\text{-adpc})][PF_6]_2$ in DMF are shown in Figures 3 and 4, respectively. The spectroelectrochemical transformations that are seen in Figures 3 and 4 are reversible; however, it should be noted that oxidation of $[\{Ru(ttp)(bpy)\}_2(\mu\text{-adpc})][PF_6]_2$ in other solvents showed poor reversibility.

In Figure 3a, the initial spectrum is that of the Ru(II,II) dinuclear complex $[\{Ru(ttp)(bpy)\}_2(\mu\text{-dicyd})]^{2+}$ in DMSO, and it is clear that at least two ν(NCN) bands are present. The spectrum of the complex $[\{Ru(ttp)(bpy)\}_2(\mu\text{-adpc})]^{2+}$ in DMSO also showed two bands, but in DMF (Figure 4) only one ν(NCN) band is observed. The observation of more than one ν(NCN) band is unusual for the solution IR spectra of dicyanamidebenzene complexes[25] but is often seen in solid state IR spectra where it has been ascribed to different conformations of the complex in the crystal lattice.[26,27] An extreme example of this is the conformation of cyanamide

(23) (a) Calvert, J. M.; Schmehl, R. H.; Meyer, T. J. *Inorg. Chem.* **1983**, *22*, 2151. (b) Berger, R. M.; McMillin, D. R. *Inorg. Chem.* **1988**, *27*, 4245.

(24) (a) Crutchley, R. J.; Naklicki, M. L. *Inorg. Chem.* **1989**, *28*, 1955. (b) Evans, C. E. B.; Ducharme, D.; Naklicki, M. L.; Crutchley, R. J. *Inorg. Chem.* **1995**, *34*, 1350.

(25) DeRosa, M. C.; White, C. A.; Evans, C. E. B.; Crutchley, R. J. *J. Am. Chem. Soc.* **2001**, *123*, 1396.

(26) Aquino, M. A. S.; Lee, F. L.; Gabe, E. J.; Bensimon, C.; Greedan, J. E.; Crutchley, R. J. *J. Am. Chem. Soc.* **1992**, *114*, 5130.

(27) Crutchley, R. J.; Hynes, R.; Gabe, E. J. *Inorg. Chem.* **1990**, *29*, 4921.

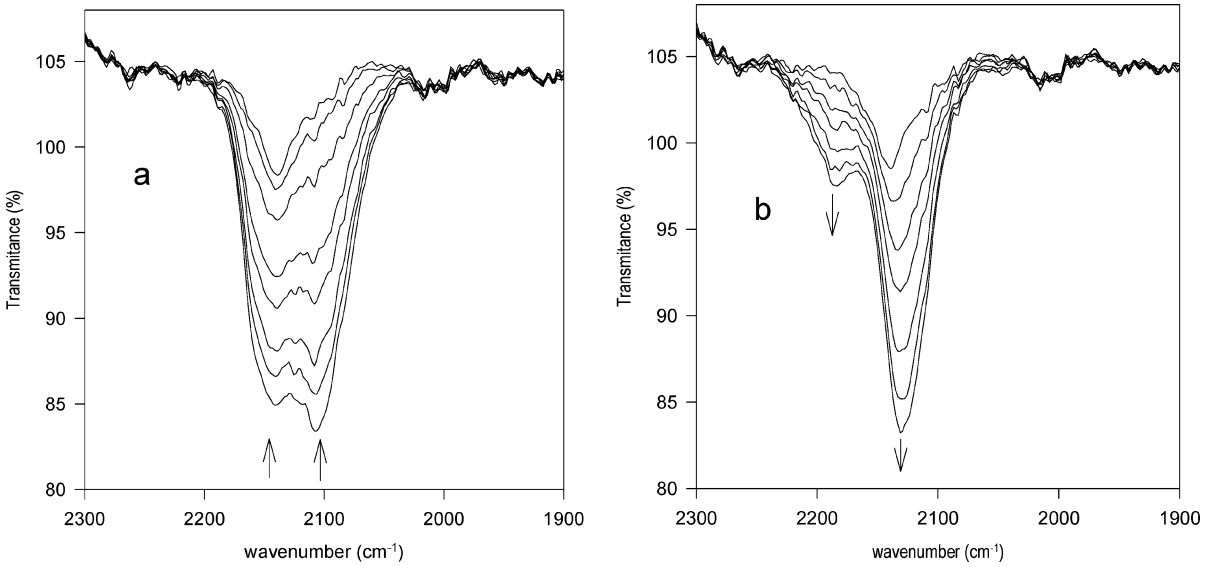

Figure 3. Infrared spectroelectrochemistry of the ν(NCN) band showing the oxidation of the Ru(II,II) complex, $[\{Ru(ttp)(bpy)\}_2(\mu\text{-dicyd})]^{2+}$, to (a) the Ru(III,II) complex and (b) the Ru(III,III) complex, in DMSO with 0.1 M TBAH electrolyte.

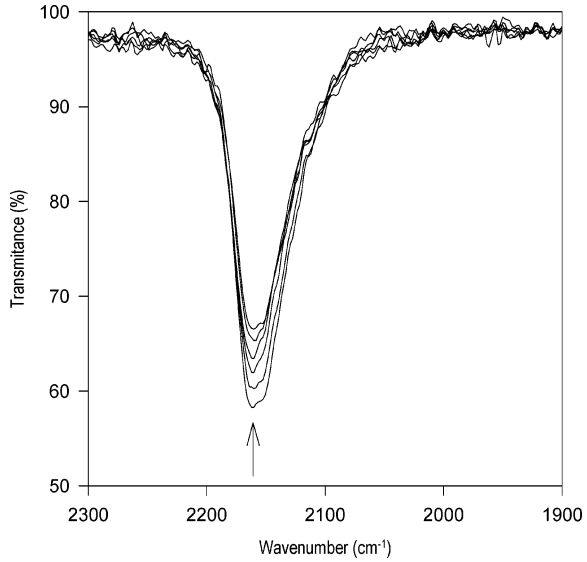

Figure 4. Infrared spectroelectrochemistry of the ν(NCN) band showing the oxidation of the Ru(III,III) complex, $[\{Ru(ttp)(bpy)\}_2(\mu\text{-adpc})]^{4+}$ to the Ru(II,III) complex in DMF with 0.1 M TBAH electrolyte.

groups of the aromatic bridging ligand. The majority of crystal structures[15,27,28] have shown a preference for the *anti* conformation, but the crystal structure of *trans,trans*-$[\{Ru(NH_3)_4(pyridine)\}_2(\mu\text{-dicyd})]^{4+}$ showed a planar bridging ligand with the cyanamide groups in a *syn* conformation.[29] We suggest that the presence of two ν(NCN) in the solution IR spectra of these complexes is an indication that both Ru(II,II) complexes exist in at least two conformations in solution.

Oxidation of both complexes to their mixed-valence form (Figure 3a and 4) showed a slight blue-shift in energy of ν(NCN) and a loss of intensity. Further oxidation of $[\{Ru(ttp)(bpy)\}_2(\mu\text{-dicyd})]^{3+}$ (Figure 3b) to give the Ru(III,III) complex showed an increase in intensity and a slight red shift in energy. An additional band appears on the high frequency side of the main ν(NCN) that we suggest is due to multiple conformations of the complex in solution. Unfortunately, the Ru(III,III) complex $[\{Ru(ttp)(bpy)\}_2(\mu\text{-adpc})]^{4+}$ is unstable, and so its IR spectrum could not be obtained.

It is important to note that the observation of only one ν(NCN) band in the IR spectra of the mixed-valence complexes $[\{Ru(ttp)(bpy)\}_2(\mu\text{-dicyd})]^{3+}$ and $[\{Ru(ttp)(bpy)\}_2(\mu\text{-adpc})]^{3+}$ is strong evidence that these complexes are delocalized on the infrared time scale (10^{13} s^{-1}).

The electronic absorption spectra of $[\{Ru(ttp)(bpy)\}_2(\mu\text{-dicyd})]^{2+}$ and $[\{Ru(ttp)(bpy)\}_2(\mu\text{-adpc})]^{2+}$ were also examined by spectroelectrochemical methods. Only a single set of isosbestic points are seen for the absorbance changes associated with a given oxidation step, and these changes are for the most part reversible.[30] The oxidation of $[\{Ru(ttp)(bpy)\}_2(\mu\text{-adpc})]^{2+}$ to the Ru(III,II) complex showed poor reversibility over long time periods, and the Ru(IIII,IIII) complex was too unstable to allow its quantitative absorbance spectrum to be obtained.

Upon oxidation of $[\{Ru(ttp)(bpy)\}_2(\mu\text{-dicyd})]^{2+}$ to the mixed-valence complex (Figure 5a), an intense band grows in centered at 1100 nm. Further oxidation to the Ru(III,III) complex (Figure 5b) results in a blue-shift of this band and a slight increase in intensity. The assignment of this band for the Ru(III,III) complex is straightforward as it is a characteristic of Ru(III)−cyanamide complexes that they possess a low energy LMCT transition.[24] The assignment of the band centered at 1100 nm in the Ru(III,II) spectrum (Figure 5a) is not as simple because a single Ru(III)−cyanamide LMCT chromophore would be expected to result

(28) Evans, C. E. B.; Yap, G. P. A.; Crutchley, R. J. *Inorg. Chem.* **1998**, *37*, 6161.

(29) Rezvani, A. R.; Bensimon, C.; Cromp, B.; Reber, C.; Greedan, J. E.; Kondratiev, V.; Crutchley, R. J. *Inorg. Chem.* **1997**, *36*, 3322.

(30) Reduction of $[\{Ru(ttp)(bpy)\}_2(\mu\text{-adpc})]^{3+}$ to the Ru(II,II) complex showed only 90% recovery in DMF solution. Identification of end point was confirmed by also taking the electronic absorbance spectrum which in the case of $[\{Ru(ttp)(bpy)\}_2(\mu\text{-adpc})]^{3+}$ showed maximum growth of the intervalence band.

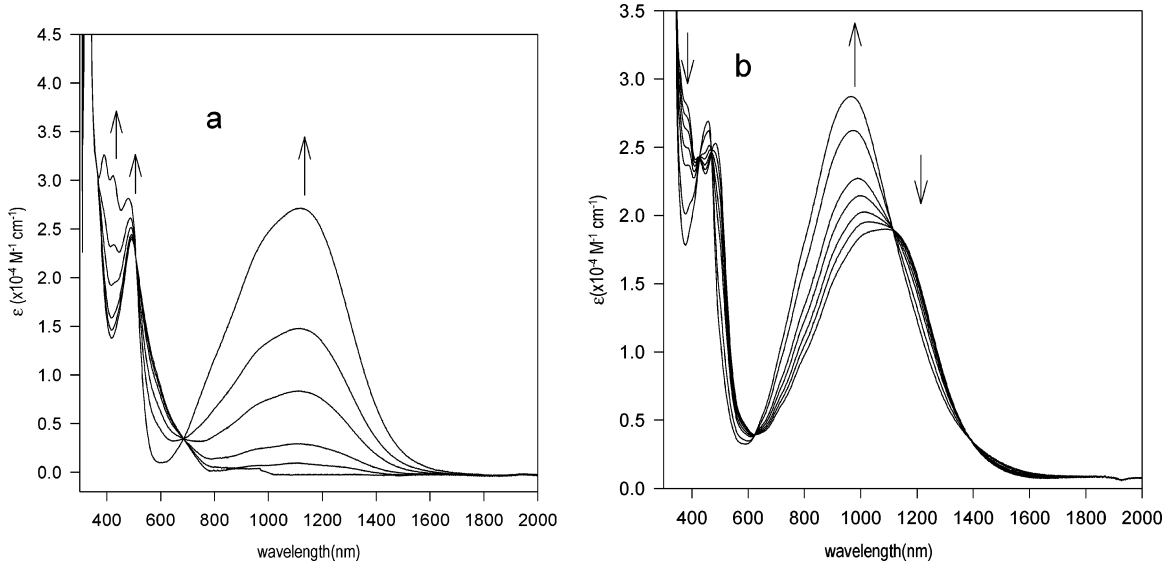

Figure 5. Spectroelectrochemical oxidation of $[\{Ru(ttp)(bpy)\}_2(\mu\text{-dicyd})]^{2+}$ to (a) $[\{Ru(ttp)(bpy)\}_2(\mu\text{-dicyd})]^{3+}$ and (b) $[\{Ru(ttp)(bpy)\}_2(\mu\text{-dicyd})]^{4+}$, in DMSO solution with 0.1 M TBAH electrolyte.

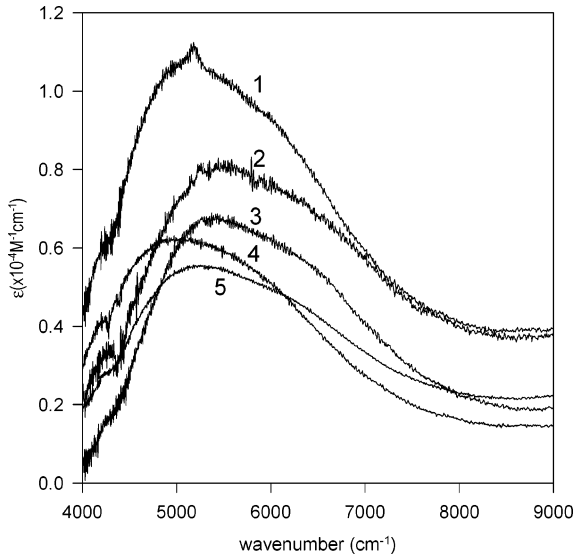

Figure 6. Solvent dependence of the intervalence band of $[Ru\{(ttp)(bpy)\}_2(\mu\text{-adpc})]^{3+}$. DMF (1), acetonitrile (2), nitromethane (3), DMSO (4), propylene carbonate (5). The spectra were generated electrochemically, with platinum working electrode, 0.1 M TBAH. The instability of the mixed-valence complex in solvents other than DMF requires that the extinction coefficient be regarded as a qualitative measure.

in a band of significantly reduced intensity compared to that seen for the Ru(III,III) complex. There is no significant absorption of the mixed-valence complex in the NIR region (up to 2600 nm), and it is suggested that the intervalence transition for this complex has combined with the LMCT transition to give the observed absorption band centered at 1100 nm. We return to this assignment in the discussion.

The spectroelectrochemical studies of the oxidation of $[\{Ru(terpyridine)(bpy)_2(\mu\text{-adpc})]^{2+}$ and that of $[\{Ru(ttp)(bpy)\}_2(\mu\text{-adpc})]^{2+}$ are not significantly different; both show a strong MMCT band at approximately 1900 nm.[15] However, the solubility of the latter complex is considerably greater, and this has allowed for a solvent dependence study of its MMCT band (Figure 6). Both chemical and electrochemical methods were used to generate the mixed-valence complex $[\{Ru(ttp)(bpy)\}_2(\mu\text{-adpc})]^{3+}$, and the energy of the MMCT band together with relevant solvent parameters have been compiled in Table 4. Unfortunately, the variation of MMCT band oscillator strength that is seen in Figure 6 is not quantitative because of the instability of the mixed-valence complex in solvents other than DMF.

Discussion

The plots of MMCT bands in Figure 6 show band shapes that are distinctly non-gaussian with a pronounced high-energy tail, and this has been mentioned as a characteristic of MMCT band properties for a delocalized complex.[13,31] Meyer has recently pointed out, for borderline delocalized mixed-valence complexes, that the asymmetry of the MMCT band may be the result of underlying metal-centered transitions due to the low symmetry of the metal ion.[6] This model predicts other low energy metal-centered transitions, and these have been observed for osmium mixed-valence complexes, but the evidence is not as clear for analogous ruthenium systems. We have attempted to find evidence for the presence of these low energy transitions in the NIR−IR spectra of our systems but have been unsuccessful. When one considers the results of the IR spectroelectrochemical study (Figures 3 and 4) and the large comproportionation constants that are seen in Table 4, it seems probable that $[\{Ru(ttp)(bpy)\}_2(\mu\text{-adpc})]^{3+}$ is not borderline but is a delocalized mixed-valence system. In this case, it is possible to explain the appearance of multiple MMCT bands by invoking a considerable degree of mixing between π-symmetry metal and nonbonding orbitals of the bridging ligand. We performed a spectroscopic analysis on the mixed-valence complexes of this study, assuming C_{2h} microsymmetry, and the results are shown in Figure 7.

In Figure 7, three MMCT transitions are symmetry allowed, $a_u \rightarrow b_g^*$ (ν_1), $b_u \rightarrow b_g^*$ (ν_2), and $a_u \rightarrow b_g^*$ (ν_3), but ν_1 is nevertheless forbidden because there is no overlap

(31) Nelsen, S. F. *Chem. Eur. J.* **2000**, *6*, 581.

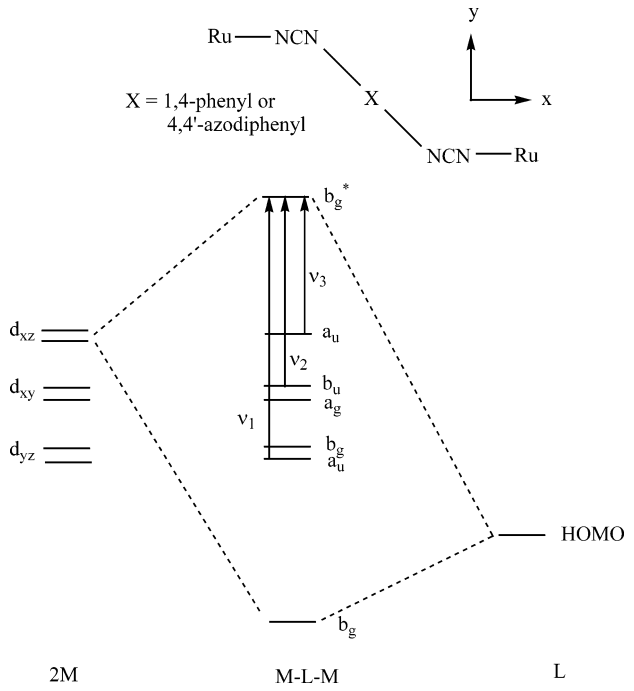

Figure 7. Qualitative molecular orbital schemes showing the origin of metal−metal transitions for the delocalized case in C_{2h} symmetry. The phenyl rings of the bridging ligands are coplanar with the *xy* plane.

between metal and ligand orbitals. Under conditions of lower symmetry, symmetry restrictions would break down, and further transitions to b_g* would be possible. In addition, IR spectroscopic and crystallographic evidence (see Results section) suggests that the complexes can exist in at least two conformations because of the *syn* and *anti* conformations of the bridging ligand. This alone would result in a doubling of observed MMCT bands. A further consequence of the treatment shown in Figure 7 is that the energy of the ν_3 transition is equal to the resonance exchange element H_{ad} for the mixing of donor, acceptor, and bridging ligand wave functions and is not equal to $2H_{ad}$ as predicted by the two-state Hush model.[1,3] Figure 7 is applicable to both [{Ru(ttp)(bpy)}$_2$(μ-adpc)]$^{3+}$ and [{Ru(ttp)(bpy)}$_2$(μ-dicyd)]$^{3+}$; however, the latter complex does not absorb significantly between 1400 and 2600 nm. There is no reason for the MMCT band of [{Ru(ttp)(bpy)}$_2$(μ-dicyd)]$^{3+}$ to be forbidden, and its energy can be predicted from comproportionation data and application of eq 5.

In Figure 2, cyclic voltammograms of the Ru(III/II) couples of the mononuclear complex [Ru(ttp)(bpy)(Cl$_4$pcyd)][PF$_6$] and the dinuclear complexes [{Ru(ttp)(bpy)}$_2$(μ-dicyd)][PF$_6$]$_2$ and [{Ru(ttp)(bpy)}$_2$(μ-adpc)][PF$_6$]$_2$, in acetonitrile solution, are shown. The Ru(III/II) couples of [{Ru(ttp)(bpy)}$_2$(μ-adpc)][PF$_6$]$_2$ are centrosymmetrically disposed about the couple of the mononuclear complex because of the approximately equal stabilization of the mixed-valence state with respect to Ru(III,III) and Ru(II,II) states of the dinuclear complex, the sum of which is the free energy of comproportionation (eq 3). This observation requires that both ΔG_{ex} and ΔG_{ip} are small for this complex. For [{Ru(ttp)(bpy)}$_2$(μ-dicyd)]$^{3+}$, the contribution of ΔG_{ex} must be accounted for because of antiferromagnetic exchange which stabilizes the Ru(III,III) state relative to the mixed-valencestate and causes the Ru(III,III)/Ru(III/II) couple to shift toward more negative potentials. This effect is clearly shown in Figure 2 where the Ru(III/II) couples of [{Ru(ttp)(bpy)}$_2$(μ-dicyd)][PF$_6$]$_2$ are not symmetrically disposed about the Ru(III/II) couple of the mononuclear complex, [Ru(ttp)(bpy)(Cl$_4$pcyd)][PF$_6$]. As antiferromagnetic exchange only affects the Ru(III,III) state, the free energy of antiferromagnetic exchange can be estimated by assuming that, in the absence of antiferromagnetic exchange, the free energy of comproportionation would be equal to twice the difference between the Ru(III,II)/Ru(II,II) couple of [{Ru(ttp)(bpy)}$_2$(μ-dicyd)][PF$_6$]$_2$ and the Ru(III/II) couple of the mononuclear complex. Subtracting the experimental ΔG_c from this calculated value of ΔG_c leads to a value of $\Delta G_{ex} = 1.08$ V or 8700 cm^{-1}. Experimental values of ΔG_{ex} for pentaammineruthenium dinuclear dicyd^{2-} complexes have approached values of 500 cm^{-1}, and so, this magnitude of ΔG_{ex} estimated for [{Ru(ttp)(bpy)}$_2$(μ-dicyd)]$^{4+}$ must reflect the greater stabilization of Ru(III) orbitals in a pentapyridine relative to a pentaammine coordination sphere.[9,26,32] The closer in energy Ru(III) orbitals are relative to π nonbonding orbitals of dicyd^{2-}, the larger the metal−ligand coupling element will be between Ru(III) and dicyd^{2-}.[32]

From the difference in resonance exchange between [{Ru(ttp)(bpy)}$_2$(μ-dicyd)]$^{3+}$ and [{Ru(ttp)(bpy)}$_2$(μ-adpc)]$^{3+}$, it is possible to estimate the energy of the MMCT band of [{Ru(ttp)(bpy)}$_2$(μ-dicyd)]$^{3+}$. Consider the equation for the free energy of resonance exchange for the symmetric delocalized mixed-valence case (eq 5). Both complexes are expected to have approximately the same thermal barrier to electron transfer because of their similar coordination spheres.[12] Subtracting ΔG_c of [{Ru(ttp)(bpy)}$_2$(μ-adpc)]$^{3+}$ from ΔG_c in the absence of antiferromagnetic exchange of [{Ru(ttp)(bpy)}$_2$(μ-dicyd)]$^{3+}$ and correcting for the number of moles of mixed-valence complex generated in the comproportionation equilibrium will yield the difference in resonance exchange between the complexes (0.39 V or 3140 cm^{-1}).[33] Adding this energy to the energy of the MMCT band of [{Ru(ttp)(bpy)}$_2$(μ-adpc)]$^{3+}$ yields a predicted MMCT energy for [{Ru(ttp)(bpy)}$_2$(μ-dicyd)]$^{3+}$ of 8700 cm^{-1}. This places the MMCT band of [{Ru(ttp)(bpy)}$_2$(μ-dicyd)]$^{3+}$ under the LMCT band centered at 1000 nm (Figure 5b) as has been previously assumed.[14]

Implicit in the construction of the molecular orbit scheme in Figure 7 is that the mixed-valence system is a delocalized case. The classical view of a delocalized system is that it should be largely insensitive to the nature of the solvent, and indeed, the comproportionation data of [{Ru(ttp)(bpy)}$_2$(μ-dicyd)][PF$_6$]$_2$ (Table 4) show no clear evidence of solvent dependence. On the other hand, the comproportionation data of [{Ru(ttp)(bpy)}$_2$(μ-adpc)][PF$_6$]$_2$ (Table 3) show a significant solvent dependence as does the MMCT band data in

(32) Naklicki, M. L.; White, C. A.; Plante, L. L.; Evans, C. E. B.; Crutchley, R. J. *Inorg. Chem.* **1998**, *37*, 1880.

(33) The nonresonance exchange contributions (ΔG_s, ΔG_i, and ΔG_e) are small relative to the free energy of resonance exchange (see ref 9) and are expected to be similar for both complexes.

Table 5. Solvent Properties and Intervalence Band Data for $[\{Ru(ttp)(bpy)\}_2(\mu\text{-adpc})]^{3+}$

solvent	$1/D_{op} - 1/d_s$	donor number	E_{IT} (cm^{-1}) by oxidant	E_{IT} (cm^{-1}) by electrochem
DMSO	0.4372	29.8	4970	4975
DMF	0.4637	26.6	5107	5181
AC	0.4934	17	5470	
PC	0.4811	15.1	5252	5254
AN	0.5289	14.1	5530	5564
NB	0.3851	4.4	5144	
NM	0.4978	2.7	5461	5373
DCE	0.3809		5420	

Table 5. This is surprising as the IR spectroelectrochemical study (Figure 4) shows that the cyanamide groups are equivalent, and this requires thermal electron transfer to be greater than the IR time scale (10^{13} s^{-1}) and therefore faster than solvent relaxation rates (10^{12} s^{-1}). In addition, a comparison of MMCT band energies derived from chemical and electrochemical oxidations in various solvents (Table 5) shows little or opposing effects. This is not expected for a valence trapped mixed-valence system in the presence of 0.1 M TBAH electrolyte.[34] What then is the mechanism by which solvent can influence the properties of $[\{Ru(ttp)(bpy)\}_2(\mu\text{-adpc})]^{3+}$ that is independent of solvent dynamics? To be consistent with all the evidence, the mechanism must be a ground-state perturbation of metal−metal coupling of a delocalized system.

The pyridine moieties of terpyridine and bipyridine ligands are fairly effective at shielding the ruthenium ion from the influence of solvent, but this is not true of the bridging $adpc^{2-}$ ligand. While the cyanamide groups of $adpc^{2-}$ are coordinated to ruthenium, the electron-acceptor azo group is exposed to the solvent, and it's electronic structure can be perturbed by the solvent's electron donor properties. Other researchers found that reducing the azo group in the bridging ligand, 4,4′-azo-dipyridine, had the effect of eliminating metal−metal coupling in the mixed-valence complex $[\{(NH_3)_5Ru\}_2(\mu\text{-}4,4'\text{-azo-dipyridine})]^{5+}$, and indeed, these authors suggested that this was a demonstration of a molecular switching device.[35] The solvent−azo, donor−acceptor interactions are not as extreme as chemical reduction, but they also apparently perturb the electronic structure of the azo group and hence the superexchange pathway in a manner that is detrimental to metal−metal coupling. This is illustrated by Figure 8 which shows the MMCT band energy (or according to Figure 7, H_{ad}) of $[\{Ru(ttp)(bpy)\}_2(\mu\text{-adpc})]^{3+}$ decreasing with increasing donor number of the solvent. The correlation is not good, and this indicates that other factors beside the donor properties of the solvent are important.

Summary

The Hush model, in which donor and acceptor mixing generates ground and excited state descriptions, is not appropriate for the mixed-valence complexes of this study. Instead, a minimum requirement is to invoke mixing of at least one bridging ligand orbital (the preferred superexchange pathway) with ruthenium donor and acceptor orbitals. The predicted metal-to-metal transition is formally assigned to a nonbonding to antibonding metal orbital transition, and the energy of this transitions is equivalent to the resonance exchange integral H_{ad}. This model can result in multiple MMCT transitions by including other metal orbitals, particularly if symmetry constraints are relaxed. In addition, this model together with comproportionation data and theory can be used to predict the energy of MMCT transitions. For $[\{Ru(ttp)(bpy)\}_2(\mu\text{-dicyd})]^{3+}$, the MMCT transition energy was predicted to be 8700 cm^{-1} which places this transition under the LMCT band envelope centered at 1000 nm.

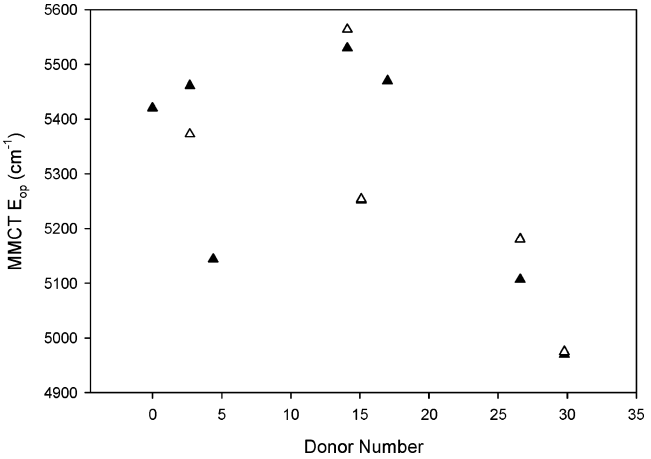

Figure 8. Solvent dependence of the energy of the MMCT band maximum of $[Ru\{(ttp)(bpy)\}_2(\mu\text{-adpc})]^{3+}$, electrochemical oxidation (△) in the presence of 0.1 M TBAH and chemical oxidation (▲) using $[Fe(bpy)_3][PF_6]_3$.

IR spectroelectrochemical studies of the cyanamide stretching frequencies of $[\{Ru(ttp)(bpy)\}_2(\mu\text{-dicyd})]^{3+}$ and $[\{Ru(ttp)(bpy)\}_2(\mu\text{-adpc})]^{3+}$ were both consistent with delocalized mixed-valence properties as were the comproportionation data. The solvent dependence of MMCT band energy that was observed for $[\{Ru(ttp)(bpy)\}_2(\mu\text{-adpc})]^{3+}$ was suggested to be largely due to a ground-state perturbation of metal−metal coupling because of a donor−acceptor interaction of solvent molecules with the azo group of the bridging ligand.

Acknowledgment. We are grateful to the Natural Sciences and Engineering Research Council of Canada (NSERC) for financial support. M.A-N. would like to thank the Hashamite University (Jordan) for a graduate scholarship.

Supporting Information Available: Full listings of crystal structure data, tables of atomic parameters, anisotropic thermal parameters, bond lengths, bond angles. Crystallographic data in CIF format. This material is available free of charge via the Internet at http://pubs.acs.org.

IC0349454

(34) Curtis, J. C.; Sullivan, B. P.; Meyer, T. J. *Inorg. Chem.* **1983**, *22*, 224.
(35) Launay, J.-P.; Tourrel-Paagis, M.; Libskier, J.-F.; Marvaud, V.; Joachim, C. *Inorg. Chem.* **1991**, *30*, 1033.